KSME

Springer

Journal of Mechanical Science and Technology 36 (10) 2022

Original Article
DOI 10.1007/s12206-022-0940-x

Keywords:
· CFD
· Garment
· Heat transfer
· Cooling effect
· Sustainable personal cooling system

Correspondence to:
Fengyuan Zou
zfy166@zstu.edu.cn

Citation:
Zhang, Y., Guo, Z., Li, T., Lyu, Y., Zou, F. (2022). Heat transfer of a sustainable personal garment cooling system. Journal of Mechanical Science and Technology 36 (10) (2022) 5281~5290. http://doi.org/10.1007/s12206-022-0940-x

Received March 28th, 2022
Revised June 22nd, 2022
Accepted June 25th, 2022

† Recommended by Editor Tong Seop Kim

Heat transfer of a sustainable personal garment cooling system

Yijie Zhang[1,2], Ziyi Guo[1], Tao Li[1,3], Yexin Lyu[1,3] and Fengyuan Zou[1,3]

[1]School of Fashion Design and Engineering, Zhejiang Sci-Tech University, Hangzhou, Zhejiang 310018, P.R. China, [2]Shangyu College, Shaoxing University, Shaoxing, Zhejiang 312300, P.R. China, [3]Key Laboratory of Silk Culture Inheriting and Products Design Digital Technology, Ministry of Culture and Tourism, Zhejiang Sci-Tech University, Hangzhou, Zhejiang 310018, P.R. China

Abstract This paper provides examines sustainable personal cooling systems. The impact of micro-fan configuration and inflow airspeed was tested. First, three different types of test models-a garment with side seam micro-fans, scatter-fans, and bottom-fans, was used to analyze and compare the heat transfer characteristic. Second, a new index of convective heat transfer was used to evaluate the cooling performance of these models. Third, the selected model was calculated with three different inflow properties, and the performance of efficiency and energy saving was analyzed. The results show that the bottom-fans model yields the best performance both on efficiency and cooling effect. The evaluation of thermal environment shows that the defined indexes are reliable to reflect heat transfer characteristics in the air gap. The comparison study of different airspeeds shows that the inflow air velocity should be set at a suitable range due to the view of energy saving.

1. Introduction

In the case of ordinary clothing, the major source of cooling to the body is provided with ventilation and evaporation holes for heat and sweat dissipation. Obviously, people may be exposed to polluted air while wearing ordinary clothing under polluted air. As the COVID-19 continues to spread, protective clothing is widely used for medical workers and volunteers because they may contact with patients and potential virus carriers. Unfortunately, body cooling by air ventilation is difficult to achieve for an enclosed protective clothing. Heat storage and wetness would cause an increase in torso body thermal discomfort, even heat stroke [1]. Therefore, a major concern in protective clothing today is to enhance its comfortability and improve its security, and aesthetics also need to be considered in some scenarios. A possible way is to design a personal garment cooling system to improve microclimate and supply clean air directly to the body surface to maintain thermal comfort, as well as to filter and purify the air which blows into the air gap between body and clothing [2].

There is a considerable amount of literature on sustainable personal garment cooling systems. Ernst and Garimella [3] developed a wearable cooling system consisting of an engine-driven vapor compression system assembled in a backpack configuration, and argued that heat removal rates of up to 300 W can maintain comfort at an activity level. Zhao and Gao [4] studied the local cooling of garments with ventilation fans and examined the cooling performance by moving the fan locations. The authors insisted that the ventilation location had a significant difference on localized intra-torso cooling. Sun and Jasper [5] investigated a 2D garment cooling system with a series of micro-fans in the side seam, and suggested that the convective cooling system can improve the convective heat transfer coefficients significantly. Choudhary et al. [6] developed a three-dimensional air ventilation cooling model to investigate human body heat loss numerically, and highlighted that the area-weighted torso heat loss was related to the fan' s air flow rate. Phelps et al. [7] tested the combined cooling effects by phase change materials and fans with a sweating manikin. They found that fans produced a constant

cooling power, but the phase change materials provided a limited cooling duration lower than 70 minutes. Miura et al. [8] evaluated two cooling devices for construction workers by a thermal manikin, and hold that a cooling vest has smaller cooling effect than cooling fans and the peak cooling powers continued for about 30 min. Kayacan et al. [9] designed two different types of liquid cooling garments and investigated their cooling effects comparatively, and insisted that the cooling effect will increase slightly while the water inlet temperature decreases or the flow rate is lower. Song et al. [10] designed a passive human body cooling fabric with high thermal comfort by increasing the dissipation of human thermal radiation and reducing energy absorption. The result shows that the cooling performance was better than traditional fabric even at a higher ambient temperature. Yang et al. [11] developed a cooling device with air-cooled exchanger and water pump to study the effects of local cooling at different torso parts. They determined that the local cooling of the torso can significantly improve the overall thermal sensation and thermal comfort of the subjects in a hot environment, and the upper back has the best effect. The above mentioned sustainable personal garment cooling system can be classified into several directions, such as liquid/gas cooling system, phase change cooling system and forced air ventilation cooling system. For liquid/gas cooling system, the garment is fabricated with the tubing carrying either cool air, cool water along the clothing surface. The cold medium circulates through the tubes and takes away the heat from skin. Nevertheless, this type of garment cooling system is a little weak in portable and energy saving due to affiliated tanks and pumps. For phase change cooling system, phase change materials are put in pockets and absorb heat on body surface during the process of phase changing. However, the cooling effect is decreasing while the phase change material is melting until the cooling effect is terminated. With the aim of achieving longer durations of cooling, a significant of material's weight is needed. For forced air ventilation cooling system, the cooling air is transported from ambient to body surface by fans or pumps [1]. Then, the fierce air convection and evaporation will take away the heat energy. The advantage of this type of garment cooling system is that it is portable, reusable, economical and simply manufactured. The speed and flow flux of airflows can be controlled easily by one's own, and the power supplier can be put in a pocket conveniently [4].

The main theme of the paper is to investigate the heat transfer characteristic of sustainable personal garment system, and choose a micro portable convective cooling system with energy efficient, inexpensive and enough cooling capability. The system consists of a series of filtered micro-fans with a diameter of 2 cm installed on the garment surface. These fans are connected to a small lithium battery. This system is intended to maintain thermal conditions which allow people overcome a severe environment. The above mentioned experimental analyses [5, 7, 10], have some shortcomings because they involve three-dimensional airflow characters and its mechanism, which may take significant local variations. Nowadays, the computational fluid dynamics (CFD) method has the ability of simulating three-dimensional fields around the human body, becomes an essential tool to analyze the effect of garments cooling system under protective clothing [12, 13].

2. Physical and mathematical method

2.1 Geometries models

A standard 3D female body was used and a type of fitting garment was chosen under various conditions. The surfaces of naked body were established and adjusted in virtual try-on software CLO Standalone; the detailed dimensions are shown in Table 1.

An X-type fitting clothing was constructed by body key girth points and ease allowance as follows: First, several horizontal cut planes were used to create body key girths and feature points. Second, the ease allowance was added on the body key girths, namely, some distance was added on these body feature points, to obtain the garment feature points. Third, the garment key girth curves were created by NURBS method. Then, garment surfaces were obtained by Bezier-spine method [14]. After that, the sustainable garment cooling fans were sewn on the correct regions of the garment surface.

With the aim of obtaining the suitable design criteria for optimizing cooling effect, three kinds of garment cooling system configurations were investigated: 1) Side-fan model, is comprised of eight 2 cm fans located in the side seam of garment. 2) Bottom-fan model, has eight 2 cm fans located in round near hemline. 3) Scatter-fan model, has eight 2 cm fans located in the key girth of garment, i.e., shoulder, bust, waist and back region, as shown in Fig. 1(b).

2.2 Mathematical models

The coupled Reynolds averaged Navier-Stokes equations (RANS) and radiative transfer equation (RTE) were applied for modelling the airflow conductive, convective and radiative heat transfer and air circulation in the air gap. The RANS equations were closed by the widely used realizable k-ε model, which is expressed as [2, 15]:

$$\frac{\partial}{\partial x_j}(\rho u_j) = 0\,, \tag{1}$$

$$\frac{\partial(\rho u_i u_j)}{\partial x_j} = -\frac{\partial p}{\partial x_i} + \frac{\partial}{\partial x_j}\left[\mu\left(\frac{\partial u_i}{\partial x_j} + \frac{\partial u_j}{\partial x_i}\right) - \rho\overline{u_i^* u_j^*}\right], \tag{2}$$
$$+\rho\beta\left(T - T_0\right) g_i$$

Table 1. Basic dimensions of 3D mannequin and clothing.

Position (cm)	Bust girth	Waist girth	Hip girth	Vertical length
Body	82	62	92	80
Clothing	86	68	98	80

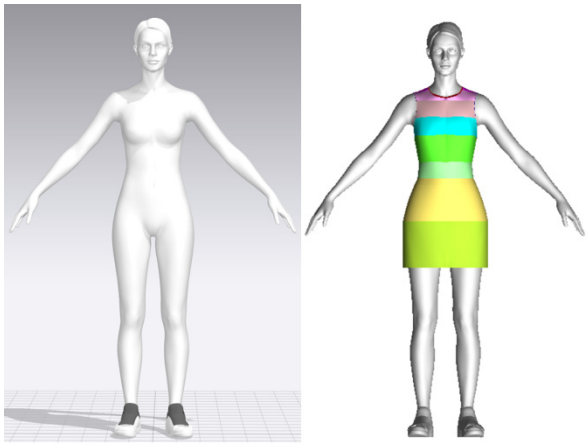

(a) Human body and garment models

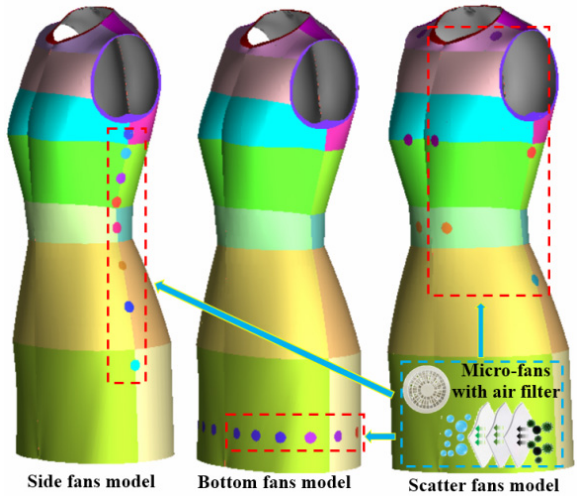

(b) Three types of micro-fans model

Fig. 1. 3D physical models and micro-fan's configurations.

$$\frac{\partial(\rho u_i c_p T)}{\partial x_i} = -\frac{\partial}{\partial x_i}\left(k\frac{\partial T}{\partial x_i} + \rho\overline{u_i} c_p \overline{T}\right), \tag{3}$$

And the realizable *k-ε* turbulence model is illustrated as:

$$\begin{aligned}\frac{\partial}{\partial x_i}(\rho k u_i) &= \frac{\partial}{\partial x_j}\left[\left(\mu + \frac{\mu_t}{\sigma_k}\right)\frac{\partial k}{\partial x_j}\right] \\ &+ \frac{\mu_t}{2}\left(\frac{\partial u_i}{\partial x_j} + \frac{\partial u_j}{\partial x_i}\right) - \rho\varepsilon\end{aligned}, \tag{4}$$

$$\begin{aligned}\frac{\partial}{\partial x_i}(\rho\varepsilon u_i) &= \frac{\partial}{\partial x_j}\left[\left(\mu + \frac{\mu_t}{\sigma_\varepsilon}\right)\frac{\partial \varepsilon}{\partial x_j}\right] \\ &+ C_{1\varepsilon}\frac{\varepsilon}{k}\frac{\mu_t}{2}\left(\frac{\partial u_i}{\partial x_j} + \frac{\partial u_j}{\partial x_i}\right) - C_{2\varepsilon}\rho\frac{\varepsilon^2}{k}.\end{aligned} \tag{5}$$

RTE is employed here for modelling the heat radiation from body to environment, which is expressed as [16]:

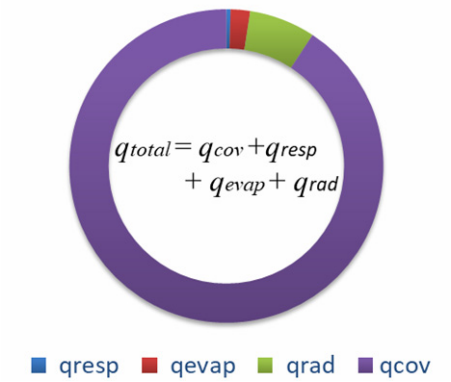

Fig. 2. Mean value of different types of heat transfer.

$$\begin{aligned}\nabla(I\hat{s}) &= \kappa\frac{\mathrm{n}^2\sigma T^4}{\pi} + I_p - (\kappa + \kappa_p + \gamma + \gamma_p) I(r,\hat{s}) \\ &+ \frac{\gamma}{4\pi}\int_{\Omega=0}^{4\pi} I(r,\hat{s}')\Phi(r,\hat{s}',\hat{s})\,d\Omega\end{aligned} \tag{6}$$

where, I_p, κ_p, γ_p are the particle equivalent emission, equivalent absorption coefficient and scattering coefficient [17].

Under an indoor situation, the human body heat loss is composed of forced convection, radiation, evaporation, and respiration:

$$q_{total} = q_{cov} + q_{rad} + q_{evap} + q_{resp} \tag{7}$$

where, q_{total} is total heat flux loss, and the q_{resp} is the respiratory heat flux, which is ignored here as it is small enough under this situation. The q_{evap} is evaporative heat flux, which is expressed as:

$$q_{evap} = \frac{w(p_{sk} - p_a)}{\mathrm{R}_{et}} \tag{8}$$

where, p_{sk} is skin vapor pressure calculated by RANS and p_a is inflow air pressure. The w, R_{et} are the skin wetness and total evaporative resistance of the garment, respectively [6]. The q_{cov} *and* q_{rad} are convective and radiative heat transfer, which were calculated by heat transfer equations: the coupled RANS and RTE. In present work, the mean q_{evap} *and* q_{rad} were found to be 23.18 W/m^2 and 78.85 W/m^2. However, the q_{cov} is higher than 650 W/m^2 on most parts of the body and the peak value reaches to 2368.1 W/m^2 due to the micro-fan's inflow air. The average value of these four types of heat transfer is shown in Fig. 2.

Therefore, to focus on forced air ventilation and convective heat transfer in the sustainable cooling system numerically, some necessary simplifications and assumptions are used [6, 16, 18]: First, because the temperature difference between body surface and ambient is small under indoor environment, the radiation heat flux is generally small and not considered in the following simulations. Second, only natural convective,

Table 2. Physical properties.

Type	Cotton	Human skin [6]	Air
Thermal conductivity (W/mK^{-1})	0.059	0.03	0.026
Thermal capacity (J/kgK^{-1})	1150	5021	1000
Density	188 g/m^2	860 kg/m^3	1.165 kg/m^3

forced convective and conductive heat transfer are considered under the indoor conditions, evaporative heat transfer is omitted as well. Third, the airflow in the air gap is treated as ideal gas with turbulence and non-compressible hypothetically. Additionally, the buoyancy effects and gravity are considered; the gravitational acceleration vector is -9.81 m/s^2.

The system of coupled RANS and RTE governing equations, along with these assumptions and boundary conditions, was successfully solved by CFD method with a commercial CFD solver CFD++. The solution was obtained by parallel computation on an Intel CORE i7 processor of 8×2.60 GHz (64 bit) and 32 GB of RAM. Double precision format was used for all kinds of computations and the converged residual level was set to below 1×10^{-5}. The global time size was set to be 5×10^{-4} s, and the run went to converging after about 6000 steps of iteration.

2.3 Mesh domain and boundary conditions

In consideration of the symmetric and computational efficiency, only half-geometry was used to generate meshes. The Ansys ICEM-CFD was used to generate the unstructured three-dimensional mesh inside the air gap. Several inflation elements were placed along the body surfaces to capture the near wall vicious flow. The generated meshes and boundary conditions are shown in Figs. 3(a) and (b).

The air flows in from micro-fans with an ambient temperature of 295 K with a constant speed of 0.4 m/s at first, and goes out around the areas of neckline and armhole. The human body is treated as an isothermal wall and the mean skin temperature is maintained at 309.8 K (i.e., 36.8 °C). Additionally, the heat transfer from garment to the outside is considered as a constant natural convection with 5 W/m^2K. The textile of sustainable garment consisted of a 100 % cotton fabric layer of thickness 0.204 mm, and the physical properties are shown in Table 2.

2.4 Methodologies evaluation

To simulate the viscous sublayer correctly, a grid independence study was held with three levels of mesh refinement [19]: namely 2.5 million nodes for crude mesh, 3.2 million nodes for medium mesh and 3.8 million nodes for refined mesh. The comparison results in Fig. 4(a) show that the dimensionless near-wall distance y+ is kept below 0.6 on the most of body surface, so the calculation precision is satisfied all over the body surface. Fig. 4(b) shows that the refined mesh is good enough to resolve the heat transfer in the air gap. The CFD method was validated with the microclimate and heat transfer experimental data of a 2D human limb in a ambient temperature of 10 °C, namely 283 K [20, 21]. The result in Figs. 4(c) and (d) depicts that current simulation agrees well with public results, so it is feasible to carry out the following investigation.

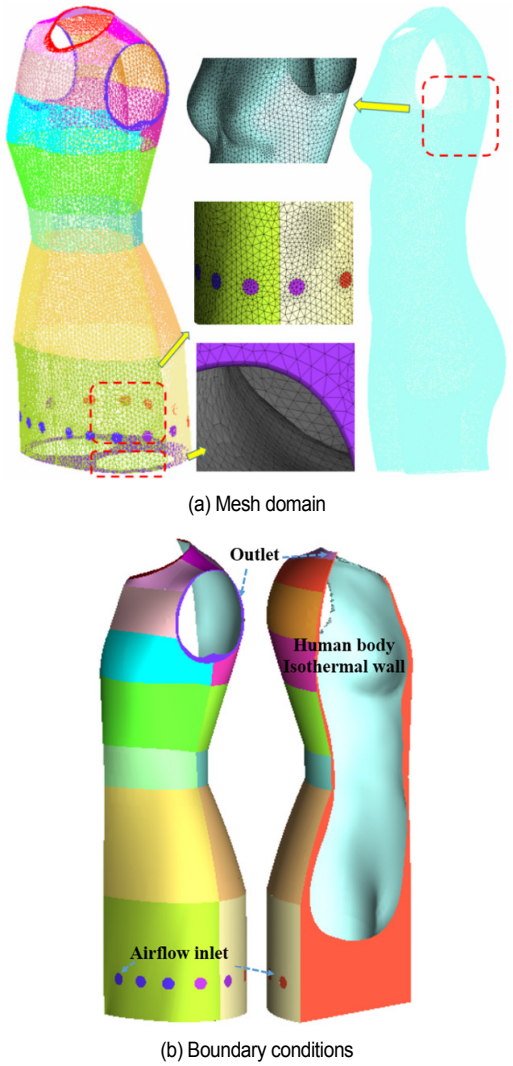

(a) Mesh domain

(b) Boundary conditions

Fig. 3. Surfaces mesh domain and boundary conditions.

3. Results and discussions

To analyze the heat transfer on the body surface quantitatively, four fixed key girth cross-sections were selected at the location of y = 22, 42, 58 and 69 cm. In the Cartesian coordinate system, the X, Y, Z refers to the horizontal, vertical and front side directions, as can see in Fig. 5.

To investigate the air ventilation effect under different fan arrangement, three kinds of simulation cases, namely side-fan, bottom-fan and scattered fan, were carried out with the constant inflow velocity of 0.45 m/s. The heat transfer coefficient, i.e., C_H, which is defined as [22]:

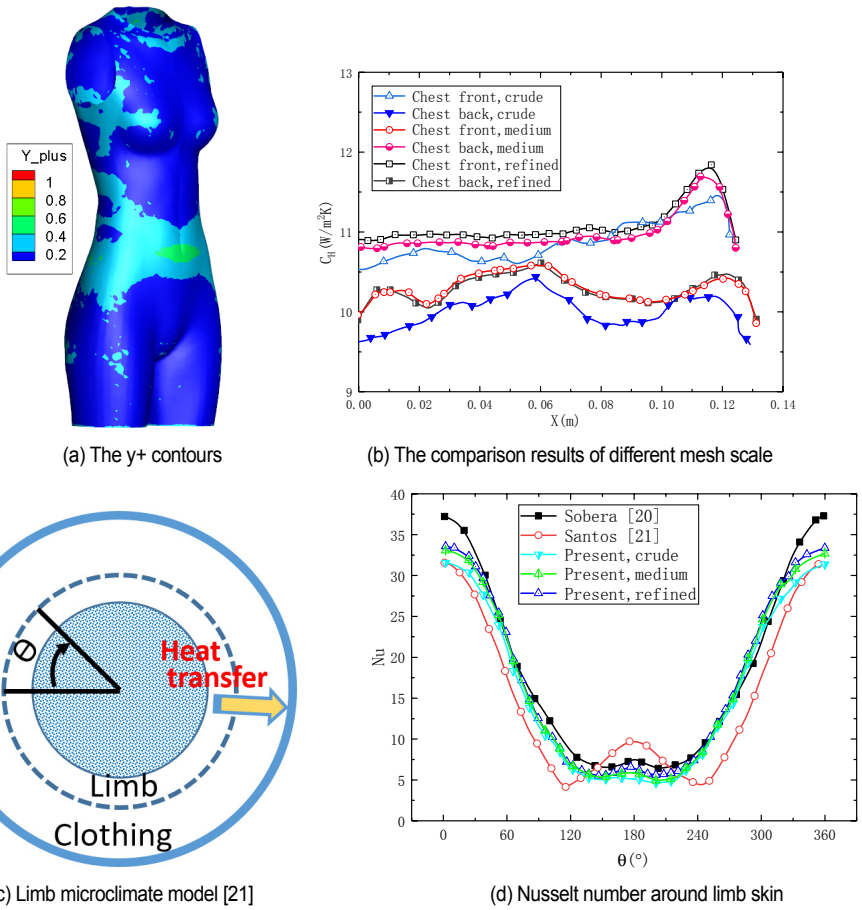

(a) The y+ contours

(b) The comparison results of different mesh scale

(c) Limb microclimate model [21]

(d) Nusselt number around limb skin

Fig. 4. Mesh check and method evaluation.

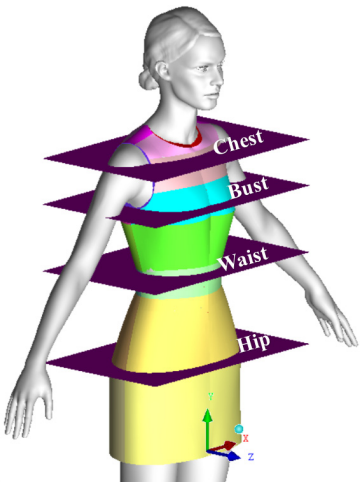

Fig. 5. Key girth cross-sections.

$$C_H = Q/(T_{wall} - T_\infty) \tag{9}$$

where, Q and T_{wall} are the surface heat flux and temperature, $T\infty$ is inflow temperature, namely, 295 K. The obtained maximum heat transfer on body key girths is shown in Table 3. As one can see, the mean value of heat transfer efficient is enhanced while the micro-fan configuration changes from side to scatter configuration, about 20 %, and is increased sharply while changed to bottom configuration on all the key girths.

3.1 Effect of micro-fan configuration

The simulated heat transfer contours of different micro-fan models are shown in Fig. 6. As one can see in Fig. 6(a), most of the high heat fluxes are focused on the area under the micro-fans for the side-fan model because the cooling air from micro-fans is injected into the body surface directly and causes fierce heat transfer. Fig. 6(b) shows that for the scattered-fan model, the high heat flux areas are distributed in the regions near the micro-fans as well, and the peak value of heat flux is lower than that of the side-fan model, which means the heat transfer is more even over the body surface. However, the scene in Fig. 6(c) is a little different from the other two, as the high heat flux area appears on the region of the neckline, under armpit and waist, far away from the micro-fans near the bottom of the clothing. The reason is that the micro-fans of the bottom-fan model are installed in the garment surface around the hip, and the distance from the micro-fan to the leg of this model is bigger than the distance from micro-fan to the bust or

waist of other models. So the inflow air from micro-fans is flow away without blocking from the body surface.

According to the principle of comfort, efficiency, and convenience, the three different arrangements of micro-fans are compared with each other. As shown in Fig. 7(a), the heat transfer coefficient of the side-fan model on chest girth is about 10 to 11 W/m^{2}K, and that of the scatter-fan model is around 12 W/m^{2}K. However, the C_H of the bottom-fan model is rising to about 20 W/m^{2}K. The lower heat transfer implies that the air flow was spread from the fan's holes to body surface slowly for side-fan model and scatter-fan model. Fig. 7(b) shows that the C_H curves on bust girth also have wave appearance, and the main value is keeping at 11.5 W/m^{2}K for the side-fans model and 12.4 W/m^{2}K for the scatter-fans model. However, there is a peak value, with a value of 20.7 W/m^{2}K, near the side-bust of the side-fans model. This high forced convection is caused by the injected airflow from micro-fans near the armpit, also is shown in Fig. 6(b). Fig. 7(c) depicts that the bottom-fans model yields the highest heat transfer coefficient. The heat transfer curves of the scatter-fan model are a little higher than that of the side-fan model, but the side-fan model has a peak value near the side waist, with a value of about 14.9 W/m^{2}K, also can be seen in Fig. 6(b). Fig. 7(d) shows the same scene as Fig. 7(a) except the curves maintain smoothness and without any waves. From the above analysis, we can see that compared with the side-fan model, the heat transfer efficiency will be increased if the micro-fans are scattered installed on the garment surface. The thermal condition will be improved at the same time because the heat transfer curve becomes smoother. The analysis of the bottom-fan model shows that the heat transfer of the bottom fans model is the most efficient one in the three models.

To further study the efficiency and cooling effect quantitatively, the mean value and standard deviation of C_H were calculated. The H_{mean} and H_{std} are expressed as:

$$H_{mean} = \frac{H_1 + H_2 + \ldots\ldots + H_n}{n} = \frac{\sum_{i=1}^{n} H_i}{n}, \quad (10)$$

$$H_{std} = \sqrt{\frac{(H_1 - H_{aver})^2 + (H_2 - H_{aver})^2 + \ldots\ldots + (H_n - H_{aver})^2}{n}}. \quad (11)$$

The comparison of H_{mean} and H_{std} is shown in Fig. 8. It shows that the side-fan model has the smallest mean value of H_{mean} and the biggest variance H_{std}, so the efficiency of side-fans is worst in all of the three models. Based on the cooling capability and energy consumption view, the bottom-fan model has the biggest mean heat transfer value, and yield the best performance of cooling effect due to the small variance. Additionally, from the point of convenience view, the bottom-fan model is also a superior candidate model because it is easy to sew the fans on a ribbon and attached to the hemline of clothing without any complex distributions.

Table 3. Mean heat transfer coefficient of garment cooling systems (W/m^{2}K).

Fans type	Inflow	Chest	Bust	Waist	Hip
Side-fans	0.4 m/s	10.7	11.1	9.8	10.5
Scatter-fans	0.4 m/s	12.8	14.2	11.4	11.2
Bottom-fans	0.4 m/s	20.5	20.2	19.4	19.6

3.2 Effect of inflow air speed

To study the heat transfer performance under different inflow velocity, three test cases of the bottom-fan model were carried out with inflow airspeed of 0.4 m/s, 0.8 m/s, and 1.6 m/s, namely, cases 1-3. The other parameters remained unchanged as

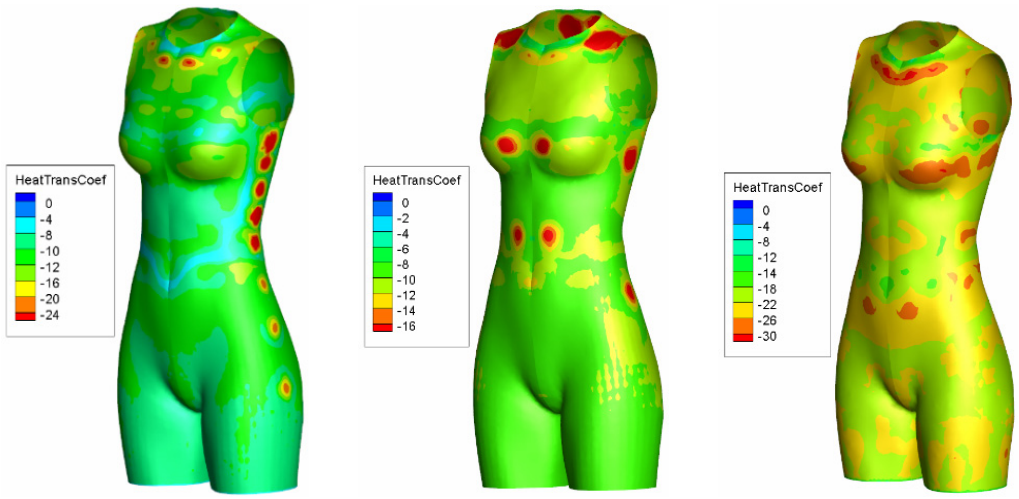

(a) Side-fans model (b) Scattered-fans model (c) Bottom-fans model

Fig. 6. Heat transfer contours on human body surface.

above mentioned. Then, the heat transfer coefficient was calculated and compared in Fig. 9. The obtained results show that the heat transfer curves rise higher while the inflow air speed is increased, which means that the heat transfer ability is increased with the increasing of inflow air velocity on the whole. It is the same that the peaks and troughs of heat flux curves become more sharp when the air-speed increases. This phenomen resulting from the more fierce forced convection heat transfer is caused by higher micro-fan's air speed. For the

Table 4. Mean heat transfer coefficient with growth rate under different air speed (W/m^{2}K).

Girth	Chest	Bust	Waist	Hip
Case 1	19.74	19.55	18.89	19.35
Case 2	21.79 (10.4 %)	21.85 (11.7 %)	20.67 (9.4 %)	21.61 (11.6 %)
Case 3	23.32 (7.0 %)	23.52 (7.6 %)	20.38 (-1.4 %)	21.94 (1.5 %)

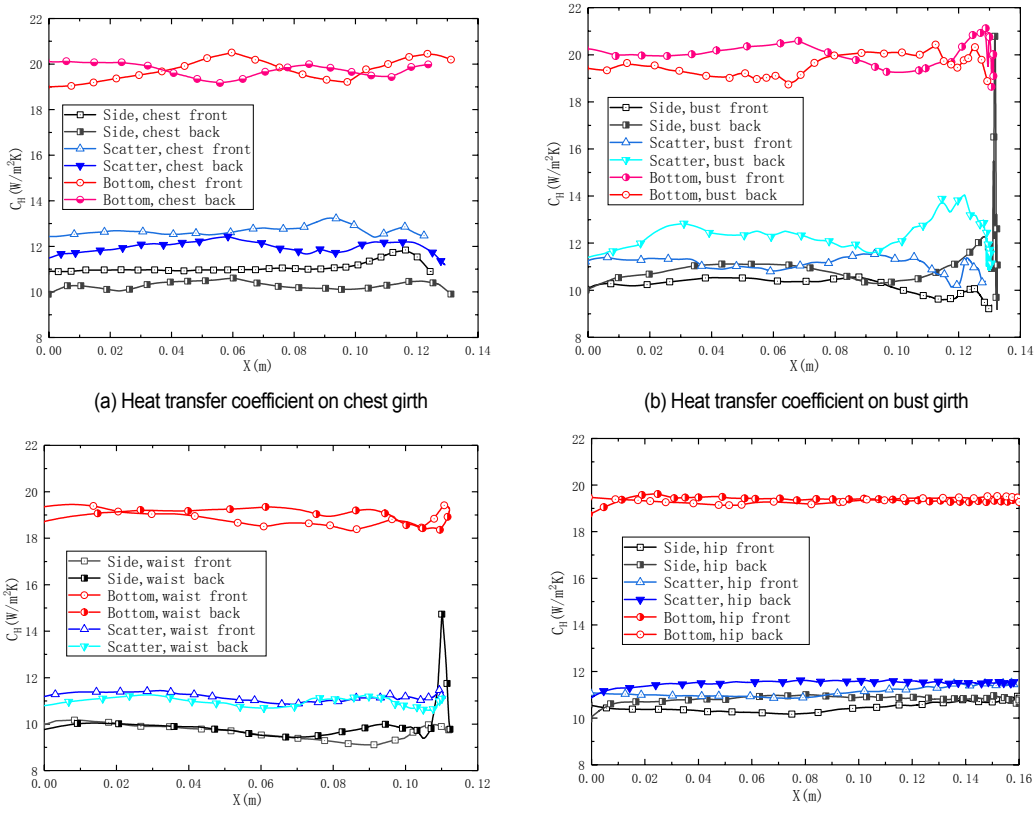

(a) Heat transfer coefficient on chest girth

(b) Heat transfer coefficient on bust girth

(c) Heat transfer coefficient on waist girth

(d) Heat transfer coefficient on hip girth

Fig. 7. Heat transfer distributions on body key girths under the condition of v = 0.4 m/s.

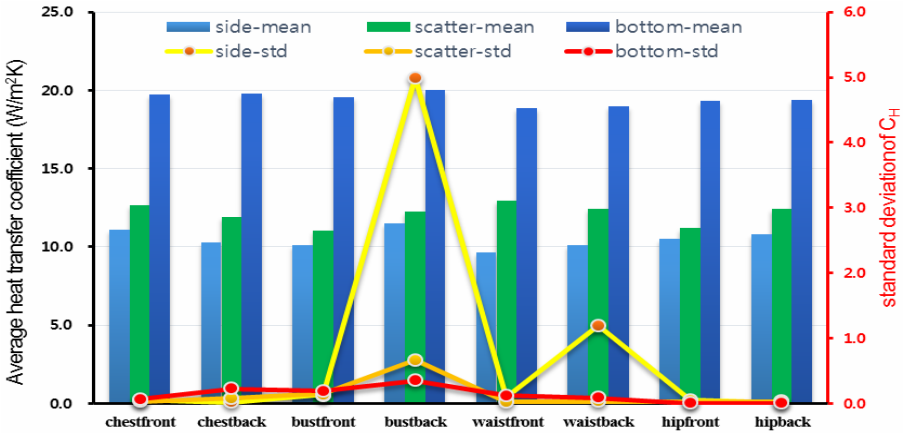

Fig. 8. Comparison of three micro-fans model.

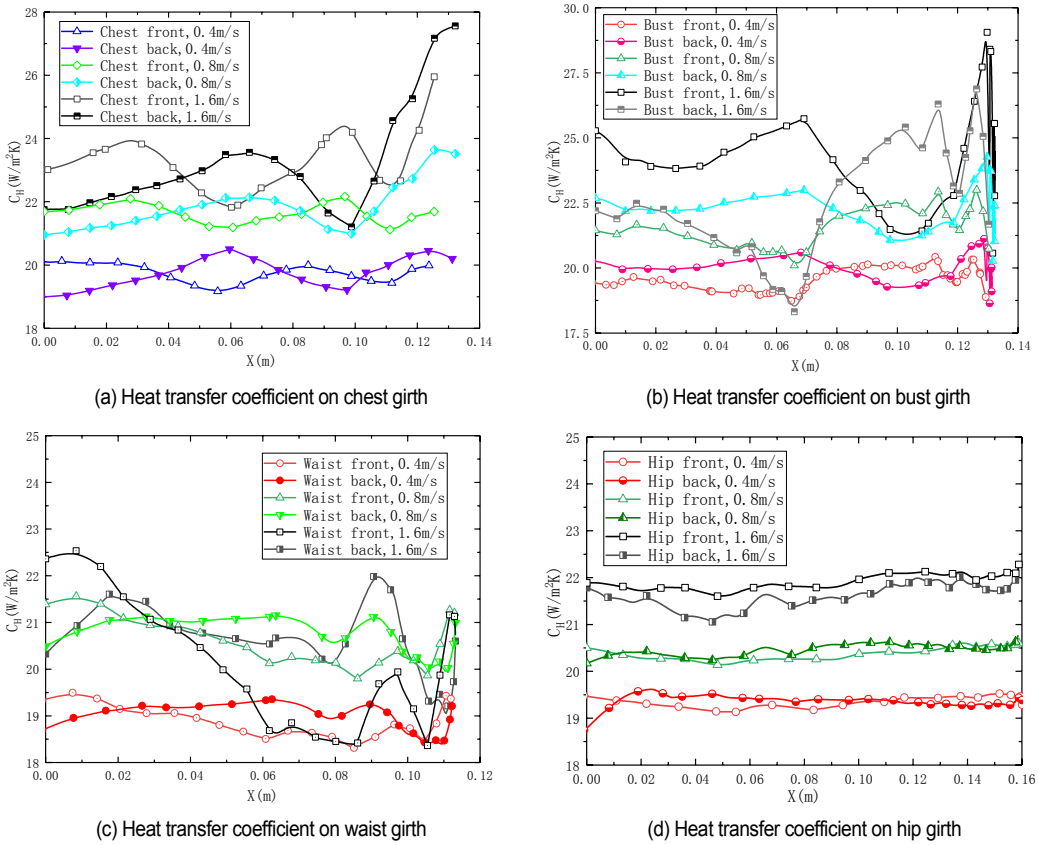

(a) Heat transfer coefficient on chest girth

(b) Heat transfer coefficient on bust girth

(c) Heat transfer coefficient on waist girth

(d) Heat transfer coefficient on hip girth

Fig. 9. Heat transfer performance under different inflow conditions.

chest girth, the mean heat transfer coefficient increased fiercely while the airspeed increased from 0.4 m/s to 0.8 m/s and 1.6 m/s. The wave appearance is shown in bust girth curves, and the fluctuation is increasing, and some peak points appear near the side bust, namely x = 0.133 m, due to the narrow air gap around the armpit. The heat transfer curves of waist girths have several ups and downs and the mean value is increased somehow. However, the curves on hip girth keep calm on the whole and the value is increased a little. These results are mainly due to the reason that the distances from clothing to leg are large enough, so the inflow air can spread to the upper body easily without any obstacle.

To study the cooling efficiency under different air speed, the heat transfer growth rates were investigated and shown in Table 4. It can be seen that in the view of cooling efficiency, the inflow air speed doubled from cases 1 to 2, as well as from cases 2 to 3, but the heat transfer coefficient just incresed a little, namely about 10 % on the whole for case 2 and under 7 % for case 3. It can be inferred from these numbers that the cooling efficiency is decreasing as the in flow speed increasing. So, from the view of energy-saving and efficiency, the inflow air velocity is not as better as higher; it should be controlled at a suitable level just sufficient for the cooling requirements. This phenomenon mainly results from the blocking of body protruding, as the air flow spreads to other body surface with high energy loss.

4. Conclusions

A major thrust of the paper was to discuss approaches and strategies for optimizing the configuration of a sustainable personal cooling system. Three different types of micro-fans systems were studied numerically, and their heat transfer abilities were compared. The results yielded some interesting findings as follows.

1) The results show that the side-fan model has the disadvantage of high temperature gradient for the side-fan model, and the scattered micro-fan can improve thermal condition due to the even heat transfer. Further, the bottom-fan model yields the best performance both on efficiency and cooling effect.

2) The evaluation index of heat transfer mean value and standard deviation results provides strong evidence that the bottom-fan model yields the best performance of thermal condition due to the small variance.

3) The comparison study of different inflow airspeeds shows that the heat transfer growth rate slows while the inflow airspeed is increased. So, the inflow air velocity should be controlled at a suitable level if energy-saving and efficiency are considered.

Nomenclature

C_H : Heat transfer efficient
CFD : Computational fluid dynamics
Q : Surface heat flux
H_{mean} : Mean value of C_H
H_{std} : Standard deviation of C_H
T_{wall} : Surface temperature
T_∞ : Inflow temperature
RANS : Reynolds averaged navier-stokes
NURBS : Non-uniform rational B-spine

References

[1] X. J. Xu and J. Gonzalez, Determination of the cooling capacity for body ventilation system, *European J. of Applied Physiology*, 111 (2011) 3155-3160.
[2] Y. J. Zhang and J. H. Jia, Numerical investigation of heat transfer in a garment convective cooling system, *Fashion and Textiles*, 9 (2) (2022) 1-14.
[3] T. C. Ernst and S. Garmella, Demonstration of a wearable cooling system for elevated ambient temperature duty personnel, *Applied Thermal Engineering*, 60 (2) (2013) 316-324.
[4] M. M. Zhao and C. S. Gao, A study on local cooling of garments with ventilation fans and openings placed at different torso sites, *International J. of Industrial Ergonomics*, 43 (3) (2013) 232-237.
[5] Y. Sun and W. J. Jasper, Numerical modeling of heat and moisture transfer in a wearable convective cooling system for human comfort, *Build and Environment*, 93 (2) (2015) 50-62.
[6] B. Choudhary, Udayraj and F. Wang, Development and experimental validation of a 3d numerical model based on CFD of the human torso wearing air ventilation clothing, *International J. of Heat and Mass Transfer*, 147 (2) (2019) 1-11.
[7] H. L. Phelps and S. D. Watt, Using phase change materials and air gaps in designing fire fighting suits: a mathematical investigation, *Fire Technology*, 55 (2) (2019) 363-381.
[8] K. Miura, K. Takagi and K. Ikematsu, Evaluation of two cooling devices for construction workers by a thermal manikin, *Fashion and Textile*, 4 (2) (2017) 23-35.
[9] O. Kayacan and A. Kurbak, Effect of garment design on liquid cooling garments, *Textile Research J.*, 80 (14) (2010) 1442-1455.
[10] Y. N. Song, R. Ma and X. Ling, Wearable polyethylene /polyamide composite fabric for passive human body cooling, *ACS Applied Material International*, 48 (10) (2018) 1-28.
[11] H. Yang, B. Cao and Y. Ju, The effects of local cooling at different torso parts in improving body thermal condition in hot indoor environments, *Energy and Building*, 198 (5) (2019) 1-23.
[12] A. Ghazy, The thermal protective performance of firefighters' clothing: the air gap between the clothing and the body, *Heat Transfer Engineering*, 38 (9-12) (2017) 975-986.
[13] Y. J. Zhang and J. H. Jia, Heat transfer in 3-D air gap between garment and body surface, *Numerical Heat Transfer, Part A: Appllication*, 79 (10-12) (2021) 708-720.
[14] D. L. Zhang, J. Wang and Y. P. Yang, Design 3D garments for scanned human bodies, *Journal of Mechanical Science and Technology*, 28 (7) (2014) 2479-2487.
[15] M. R. Haque and M. A Rahman, Numerical investigation of convective heat transfer characteristics of circular and oval tube banks with vortex generators, *Journal of Mechanical Science and Technology*, 34 (1) (2020) 457-467.
[16] Y. Zhang and J. Jia, Numerical simulation of solar radiation and conjugate heat transfer through cabin seat textile, *Autex Research J.*, 21 (4) (2021) 501-507.
[17] Y. J. Zhang, Y. X. Lyu, J. Y. Wu, T. Li and F. Y. Zou, Numerical prediction of the heat transfer in air gap of different apparel modeling, *Autex Research J.*, 22 (4) (2022) 1-8.
[18] S. Rath and K. D. Sukanta, Natural convection in power law fluids from a pair of two attached horizontal cylinders, *Heat Transfer Engineering*, 18 (2) (2020) 1-8.
[19] J. W. Seo, J. H. Park and Y. H. Choi, Numerical study on human model shape and grid dependency for indoor thermal condition evaluation, *Journal of Mechanical Science and Technology*, 27 (2) (2013) 397-405.
[20] M. P Sobera, R. Chris and Kleijn, Convective heat and mass transfer to a cylinder sheathed by a porous layer, *AIChE J.*, 49 (12) (2003) 3018-3028.
[21] M. S. Santos, D. Oliveira and J. B. Campos, Numerical analysis of the flow and heat transfer in cylindrical clothing microclimates, Influence of the microclimate thickness ratio, *International J. of Heat and Mass Transfer*, 117 (3) (2017) 71-79.
[22] Metacomp technologies inc., *CFD++ User Manual*, Agoura Hills, CA. (2013).

Yijie Zhang is a lecturer at Shangyu College, Shaoxing University, China. She received her Ph.D. in Fashion Design and Engineering from Zhejiang Sci-Tech University. Her research interests include garment digital design, body heat transfer.

Ziyi Guo is a Ph.D. student in Fashion Design and Engineering, Zhejiang Sci-Tech University, China. His research is focused on intelligent garment design technology.

Tao Li received the M.S. in Clothing Design and Engineering from Zhejiang Sci-Tech University in Hangzhou, China. He is currently a Ph.D. postgraduate in Zhejiang Sci-Tech University. His research interest is mainly in the area of clothing digitization technology.

Yexin Lyu received double Master's degrees in Fashion Design and Engineering from Zhejiang Sci-Tech University, China and in Clothing Science from Bunka Gakuen University, Japan. She is currently pursuing a Ph.D. at Zhejiang Sci-Tech University. Her current research interests include three-dimensional body shape classification and garment digitalization technology.

Fengyuan Zou is a Professor of Fashion Design and Engineering, Zhejiang Sci-Tech University, China. He is the director of Zhejiang Provincial Engineering Laboratory of Clothing Digital Technology and the director of Clothing Engineering Research Center of Zhejiang Province. His research interests include clothing digital design, intelligent clothing.